MRI of the Anal Region in Crohn's Disease and Beyond

Silvio Mazziotti, Giuseppe Cicero,
Alfredo Blandino, and Tommaso D'Angelo

Perianal involvement in Crohn's disease can be complicated by a variety of pathologic conditions [1]. Perianal abscess occurs in up to 80% of patients with CD, as the frequency of perianal fistulas varies from 17% to 43% [2–9].

The risk of perianal involvement increases when the distal gastrointestinal tract is affected. In fact, patients with disease confined to the colon have a higher incidence of perianal fistulas, and the rate can approach 100% in patients with a rectal CD localization [4, 10]. Although the precise etiology of perianal fistulas remains unknown, they may be caused by obstruction of sinus tracts or cryptoglandular infections [1]. The former theory suggests that fistulas may arise due to the extension of deep penetrating ulcers into the anus or distal rectum; over time, fecal material stagnates within the ulcers and the evacuating pressure also facilitates their further extension with formation of a real fistula [1, 11]. According to the latter theory, infection of anal glands gives rise to abscess formation which represents the point of origin of a fistula [12].

Perianal alterations may anticipate the intestinal manifestations of CD by several months or years. About two-thirds of patients with perianal disease will be diagnosed with intestinal disease within 1 year and another third within 1–5 years, with only a few patients being diagnosed after more than 5 years. Only a small proportion of patients with CD may persist in having isolated perianal involvement [13, 14].

Surgical management of perianal CD depends on the extent, localization, and complexity of the fistula. The surgical approach can be more invasive in case of large fistulas and in presence of abscesses.

Therefore, imaging is necessary for surgical planning. The main purpose is to identify the primary fistulous track, especially when a cutaneous opening is absent, the possible secondary tracks, and the sites of any abscess cavities, and to define their anatomic relation with the sphincters, the levator ani muscle, and the ischiorectal and ischioanal fossae [15].

9.1 Classification of Fistulas

Classification systems for perianal fistulizing CD disease are useful in determining what surgical procedure (if any) should be performed. Several classifications have been used to define the different types of fistulas. The most anatomically detailed and used is the one established by Parks. This classification distinguishes four different possible paths: inter-sphincteric, trans-sphincteric, supra-sphincteric, and extra-sphincteric [16]. Since there is no relation

S. Mazziotti (✉) · G. Cicero · A. Blandino
T. D'Angelo
Department of Biomedical Sciences and Morphological and Functional Imaging, University Hospital Messina, Messina, Italy
e-mail: smazziotti@unime.it; gcicero@unime.it; ablandino@unime.it; tdangelo@unime.it

between the sphincter or the perianal canal, superficial subcutaneous fistulas are excluded from Parks' classification (Fig. 9.1).

On the other hand, the St. James's University Hospital classification has been developed according to MRI findings. Fistulas are distinguished on a 5-point scale: grade 1, simple linear inter-sphincteric with no ramifications; grade 2, inter-sphincteric with presence of abscess or secondary tract bounded by the external sphincter; grade 3, external sphincter leak with trans-sphincteric path and possible hyperemia or edema arising within the adjacent fossae; grade 4, trans-sphincteric with extension to the ischio-rectal fossa where an abscess can be found; grade 5, the fistulous path extends above the supralevator ani with involvement of the ischio-rectal fossa [17].

Finally, the Standards Practice Task Force of the American Society of Colon and Rectal Surgeons has analyzed this topic from the surgical point of view. This classification merely evaluates the anal disease on the basis of the possible treatments, distinguishing simple fistula-in-ano, complex fistula-in-ano, fistulas associated to CD and abscesses [18].

9.2 Technique

MRI of the anal district is performed through a surface phased array coil without any need of lumen dilation.

The field of view must be cranio-caudally extended from the supralevator plane to the anal verge including the surrounding gluteal fat tissue [19–21].

An initial sagittal T2-weighted Turbo-Spin echo (TSE) can be obtained in order to provide an overview of the anal canal and to orientate the following scans.

The following T2-weighted TSE sequences are acquired on oblique-coronal and axial planes respectively orientated perpendicular and parallel to the major axis of the anal canal (Fig. 9.2).

The use of T2-weighted TSE scans with fat saturation significantly facilitates the detection of fluid collection and perilesional edema.

Two- or three-dimensional T1-weighted images with fat saturation obtained before and after the injection of gadolinium contrast material are useful not only for identification of fistulas, but also in distinguishing active inflammation from fibrosis. In fact, enhancement tends to be early and intense in the former condition, whereas it appears more progressive and delayed in the latter.

Finally, oblique-coronal or, preferably, oblique-axial diffusion-weighted images (DWI) highlight the presence of fistulas and abscesses and result particularly important in case of contraindications to intravenous contrast medium injection [19, 20, 22].
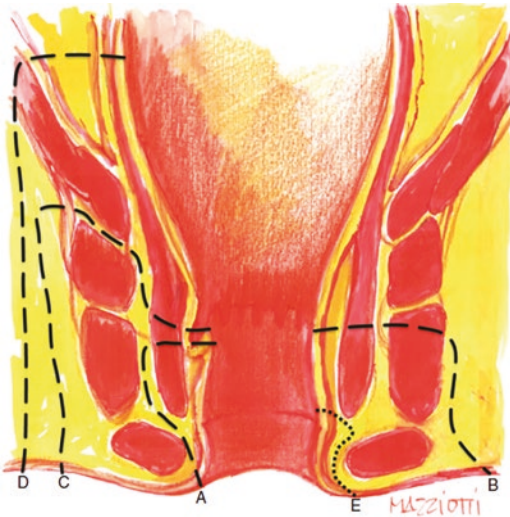
Fig. 9.1 Parks' classification: (A) Inter-sphincteric fistula, (B) Trans-sphincteric fistula, (C) Supra-sphincteric fistula, (D) Extra-sphincteric fistula, (E) Subcutaneous fistula (not part of Parks' classification)
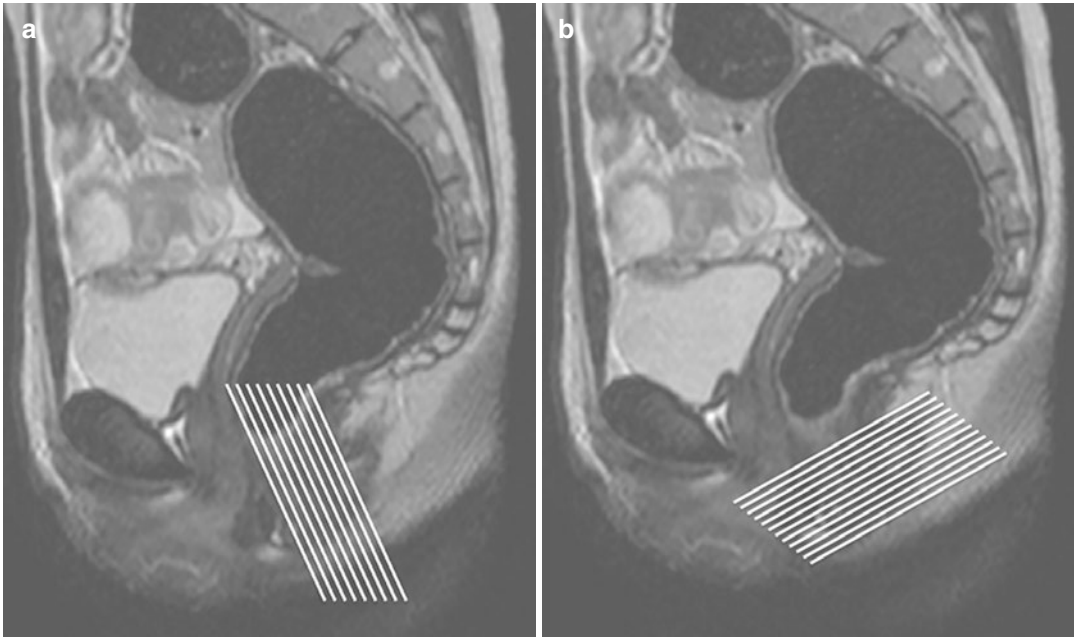
Fig. 9.2 Technique. Orientation of coronal (**a**) and axial (**b**) scan series on a midline sagittal T2-weighted TSE image, respectively, parallel and perpendicular to the major axis of the anal canal

9.3 Perianal Findings in Crohn's Disease

Active fistulous tracts and abscesses filled with pus and granulation tissue appear as hyperintense structures on T2-weighted and STIR images (Figs. 9.3, 9.4, and 9.5). In particular, identification of the tract is easier when evaluating fat-saturated sequences, whereas T2-weighted scans without fat suppression give more detailed information about the anatomic relationship of the tract with the surrounding anatomical structures (Fig. 9.6). Active tracts are often surrounded by hypointense fibrous walls, which can be relatively thick and hypointense, especially in cases of recurrent disease and/or previous surgery (Fig. 9.7). Some hyperintensity in this fibrous tissue may seldom be seen, probably due to associate inflammatory edema. This hyperintensity may also extend beyond the tract and its fibrous sleeve, reflecting adjacent inflammation (Fig. 9.8). On contrast-enhanced T1-weighted images, active fistulous tracts brilliantly enhance, as do the walls of abscess cavities (Figs. 9.3, 9.4, and 9.9). Retained pus remains unenhanced, with a resulting peripheral ring enhancement, a typical appearance of abscess elsewhere in the body.

MRI performed along the coronal and axial planes demonstrates fistulous tracks in relation to the sphincteric complex, ischiorectal and ischioanal fossae, and levator plane. Tracts are described in accordance with the terminology illustrated by Parks et al. [16].

When a fistula is contained by the external sphincter, it is defined as inter-sphincteric (Fig. 9.7). On the contrary, any evidence of a fistulous tract in the ischioanal fossa effectively excludes an inter-sphincteric fistula. Moreover, it should also be considered that trans-, supra-, and extra-sphincteric fistulas share the common feature of a tract that lies beyond the confines of the external sphincter. Although trans-sphincteric fistulas are the most common cause of a tract in the ischioanal fossa (Fig. 9.10), it must be remembered that a differentiation between these three fistulas is possible only by locating the internal
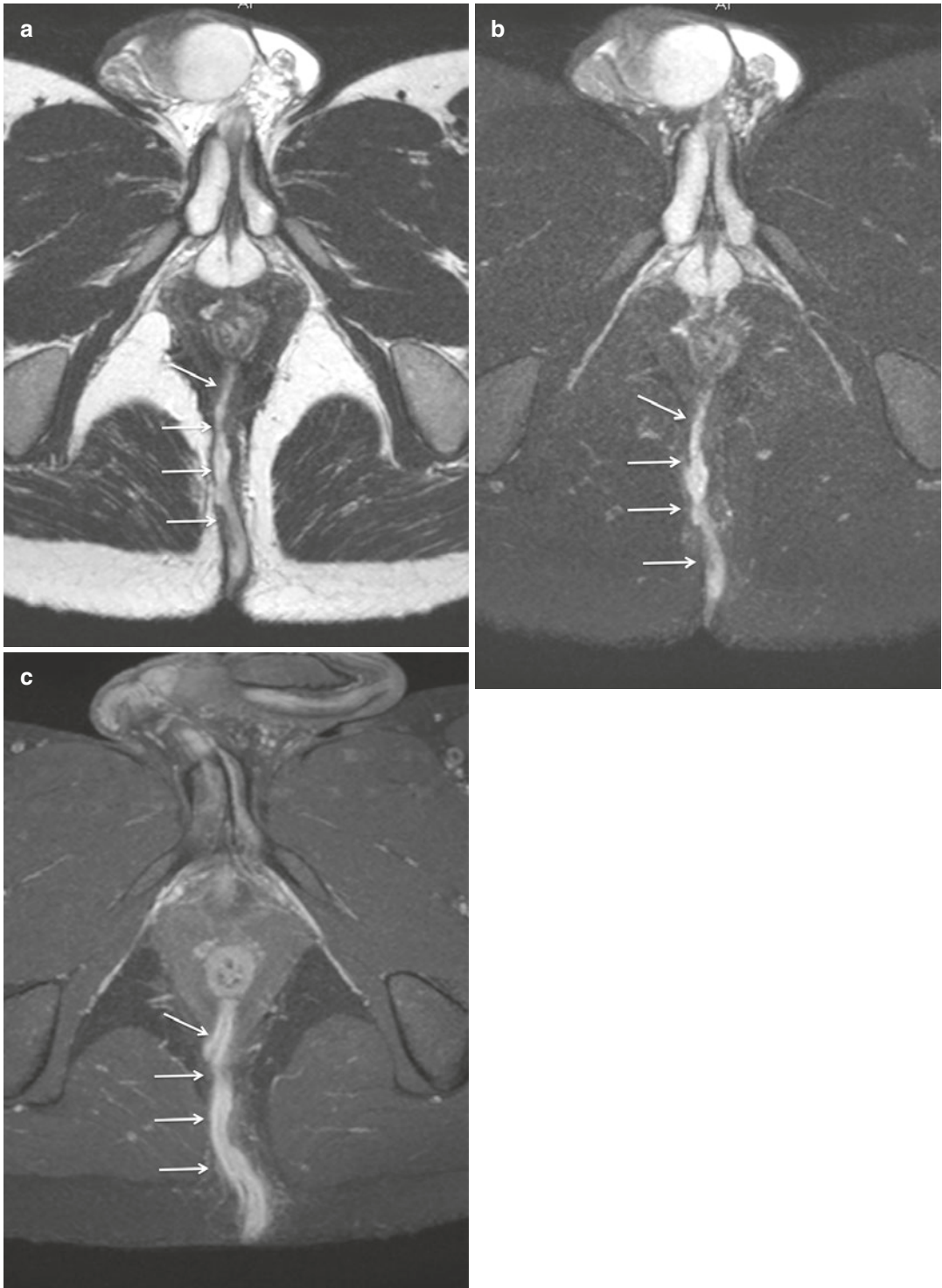
Fig. 9.3 Trans-sphincteric fistula. Axial-oblique T2-weighted TSE images performed without (**a**) and with fat saturation (**b**) show a posterior midline hyperintense trans-sphincteric fistula (arrows). Contrast enhancement of the inflamed wall of the fistula is well depicted after i.v. injection of Gadolinium (**c**)
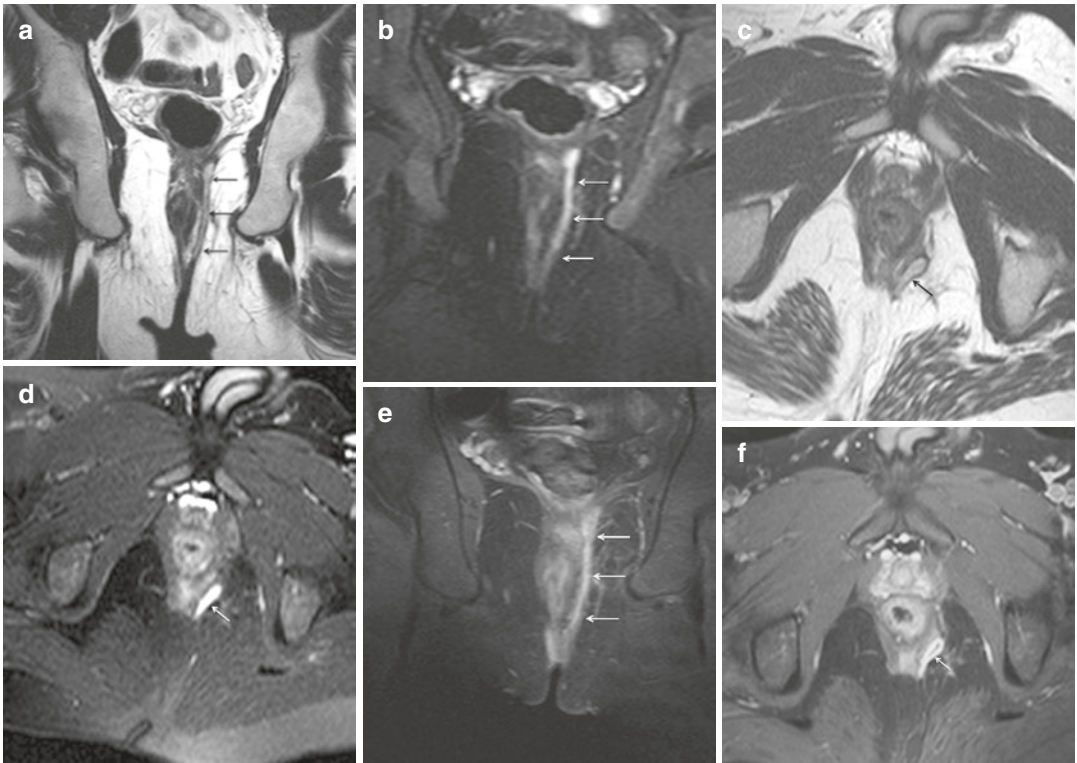
Fig. 9.4 Extra-sphincteric fistula. Coronal-oblique (**a**, **b**) and axial-oblique (**c**, **d**) T2-weighted TSE images, performed without (**a**, **c**) and with fat saturation (**b**, **d**) show a left hyperintense extra-sphincteric fistula (arrows). On coronal-oblique (**e**) and axial-oblique (**f**) T1-weighted TSE fat-saturated images, performed after Gadolinium administration, enhancement of the fistulous walls is well depicted (arrows)

opening and clearly determining the course between this and the primary tract [23].

Finally, in presence of voluminous perianal abscesses, eventual fistulous tracts can be hidden, due to the compression or dislocation of the sphincter complex itself and, in more severe cases, large dehiscence with nearby pelvic viscera may also be found (Figs. 9.11 and 9.12).

In order to describe the exact site and direction of fistulous tract according to the surgical view, radiologist should correlate the axial MRI findings to the "anal clock."

With this system, key points of the fistula, such as internal opening and path, are referred to as the sphincteric structures using clock benchmarks. Axial sequences are employed for this assessment and position of the patient inside the scanner must be clarified since it can differ from that of clinical examination or surgical intervention [20, 24].

Fig. 9.5 Trans-sphincteric fistula with abscess. Axial-oblique (**a**) and coronal-oblique (**b**, **c**) T2-weighted TSE images show a posterior midline trans-sphincteric fistula (arrows in **a**) with its course in the left ischioanal fossa (white asterisks in a and **b**). A voluminous perianal abscess can also be seen (black asterisk in **c**) with a small gas bubble in its context (arrow)
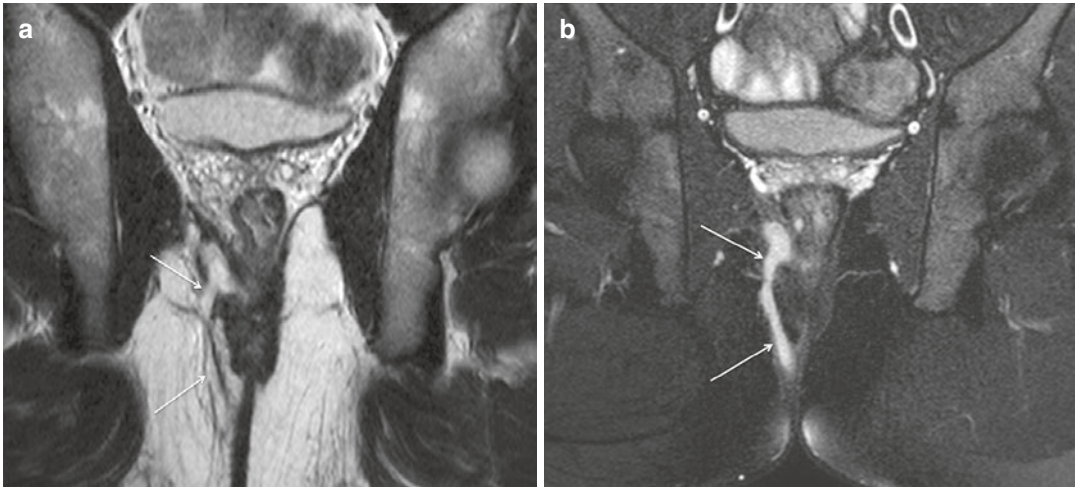
Fig. 9.6 Trans-sphincteric fistula. Coronal-oblique T2-weighted TSE image (**a**) shows a right trans-sphincteric fistula, involving the ipsilateral ischioanal fossa (arrows). Fat-saturated image (**b**) clearly shows the fistulous tract (arrows) due to suppression of fat intensity signal
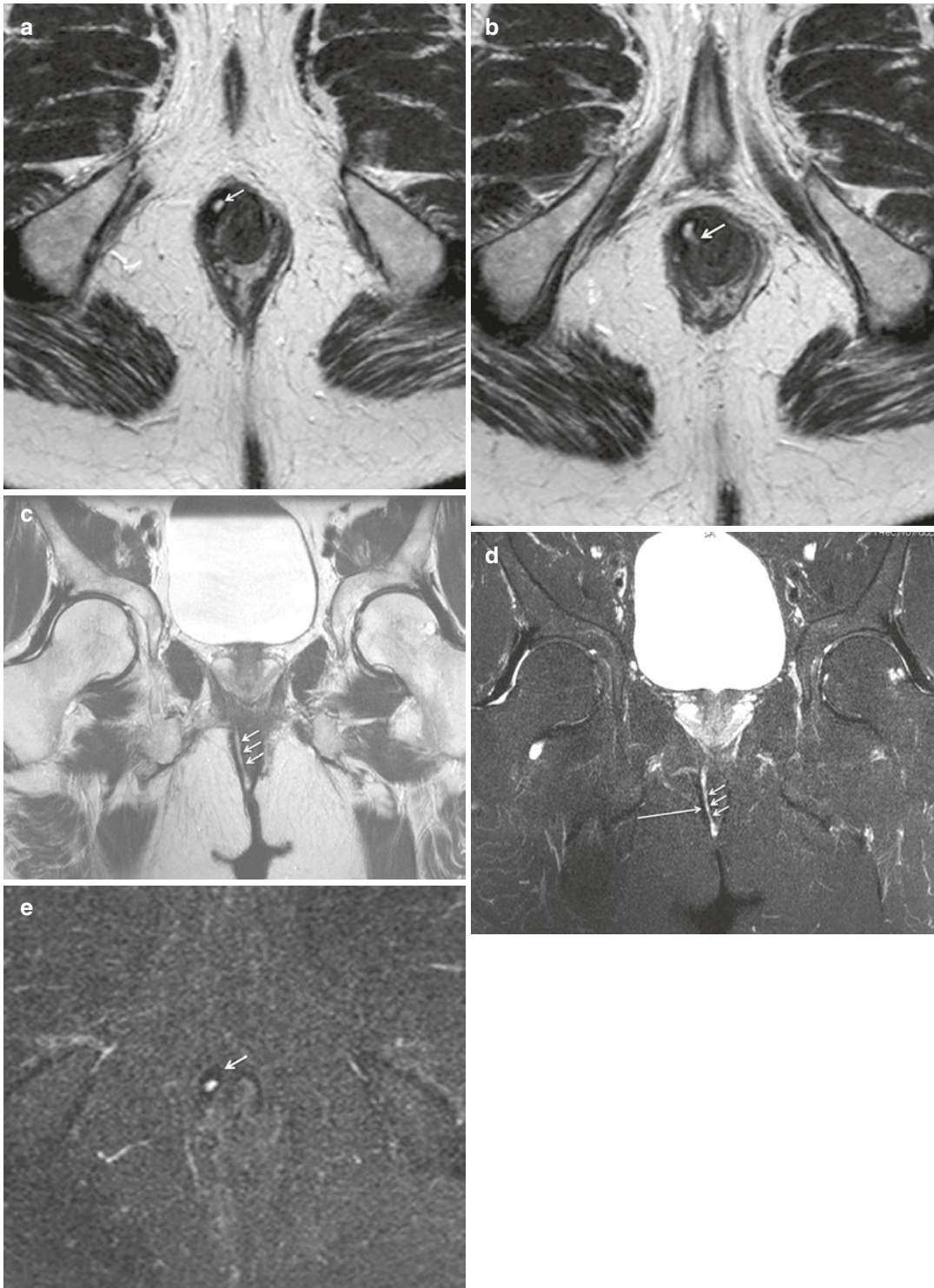
Fig. 9.7 Inter-sphincteric fistula. Axial-oblique T2-weighted TSE images (**a**) show inter-sphincteric fistula at 11 o'clock (arrow). In a more cranial image (**b**) the internal opening is demonstrable (arrow). Coronal-oblique T2-weighted TSE images performed without (**c**) and with fat saturation (**d**) show right inter-sphincteric fistula, traceable along most of its course (short arrows), with sparing of ischioanal fossa. Note the hypointense fibrous wall surrounding the active fistula (long arrow in **d**), also confirmed in the axial T2-weighted TSE fat-saturated image (**e**) obtained through its middle part (arrow)
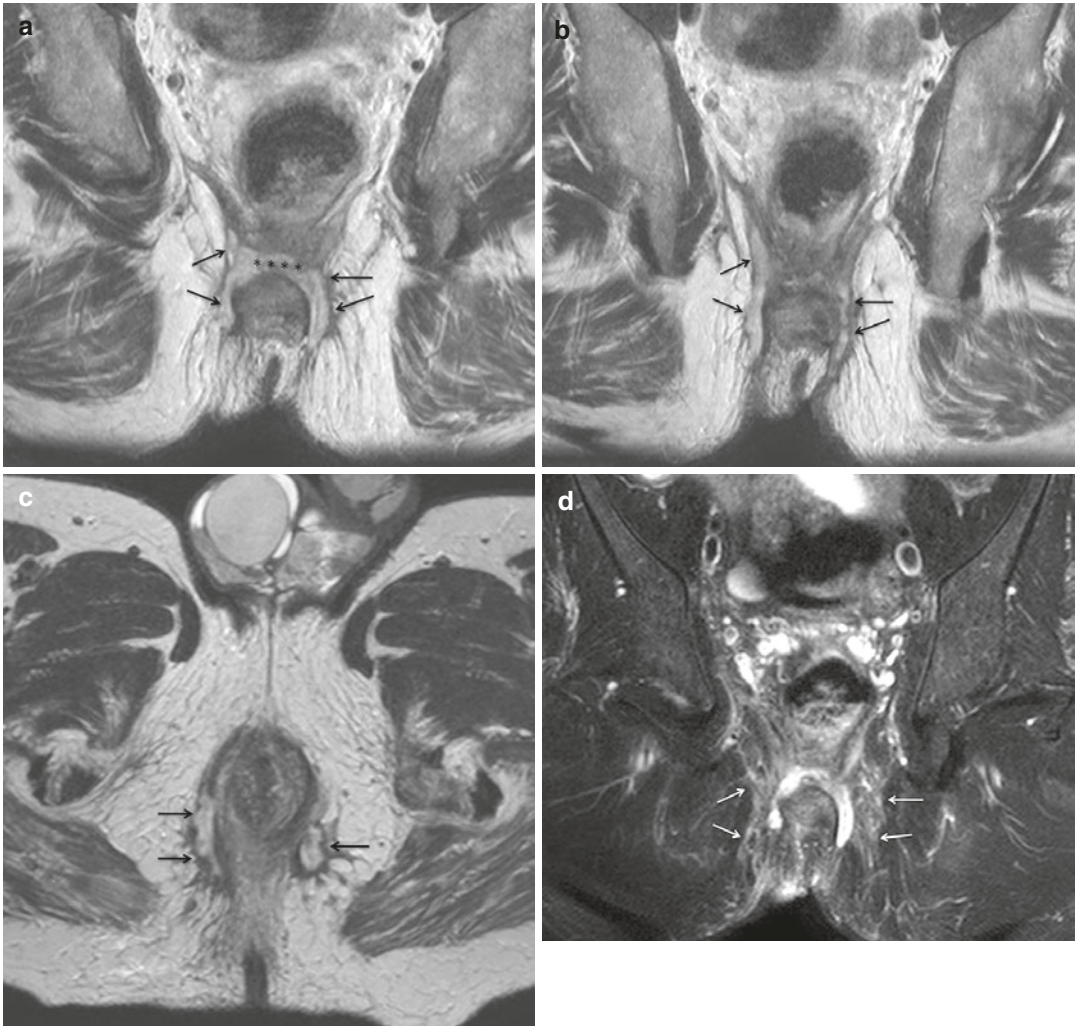
Fig. 9.8 Complex perianal fistula. Coronal-oblique T2-weighted TSE images (**a**, **b**) and axial-oblique T2-weighted TSE image (**c**) show a horseshoe-like inter-sphincteric fistulous tract (asterisks in **a**), which extent bilaterally toward ischioanal fossa through external sphincter (arrows). Coronal-oblique T2-weighted TSE fat-saturated image (**d**) well demonstrates perifistulous inflammatory edema (arrows)
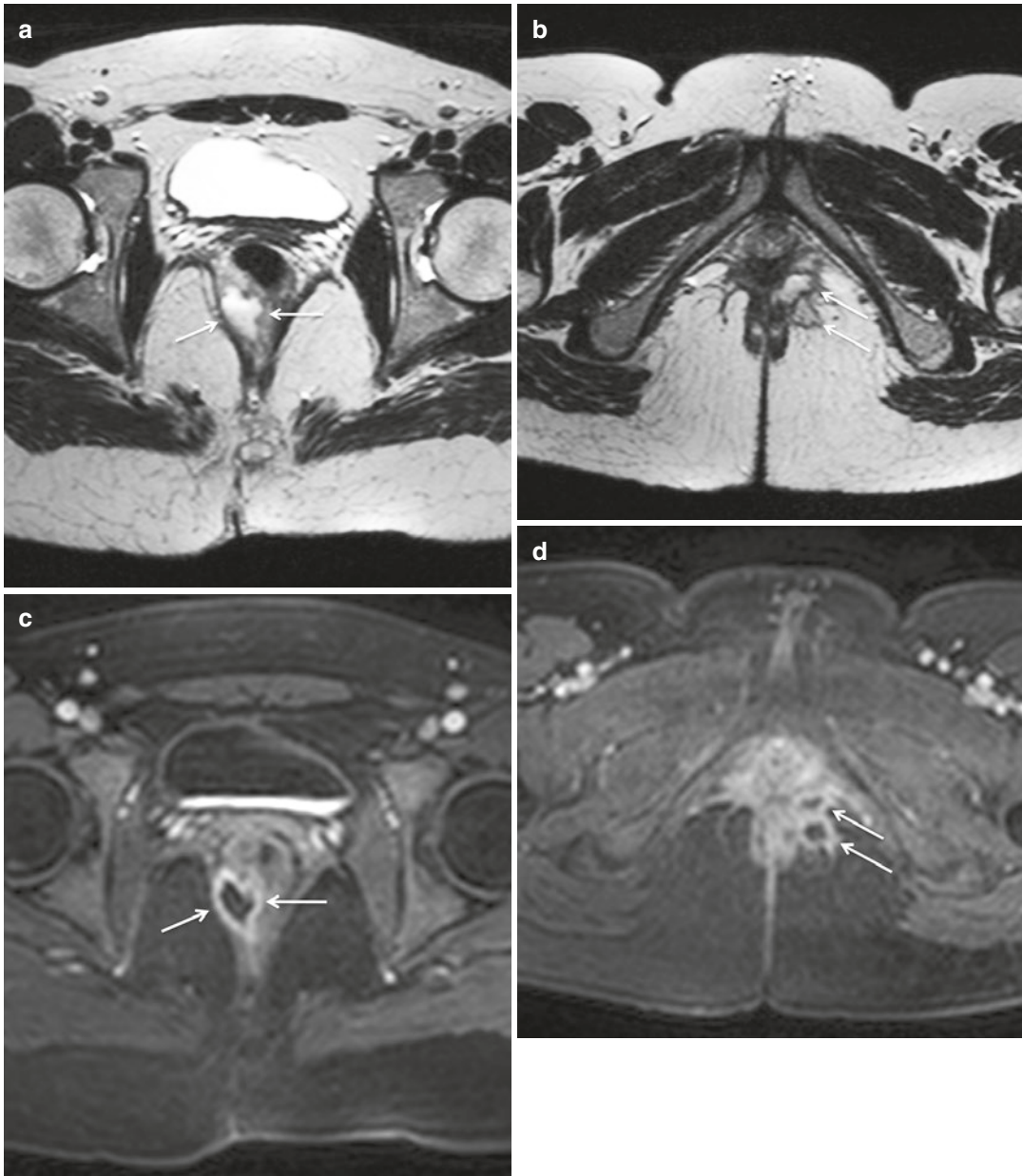
Fig. 9.9 Perianal fistula with multiple abscesses. Axial-oblique T2-weighted TSE image (**a**) shows a right-sided abscess (arrows). A more caudal scan (**b**) demonstrates other two small abscesses in the left ischioanal fossa (arrows). Axial-oblique T1-weighted TSE fat-saturated images, obtained after i.v. injection of Gadolinium (**c**, **d**) shows peripheral contrast enhancement of abscesses, containing a central component of non-enhancing purulent material (arrows)
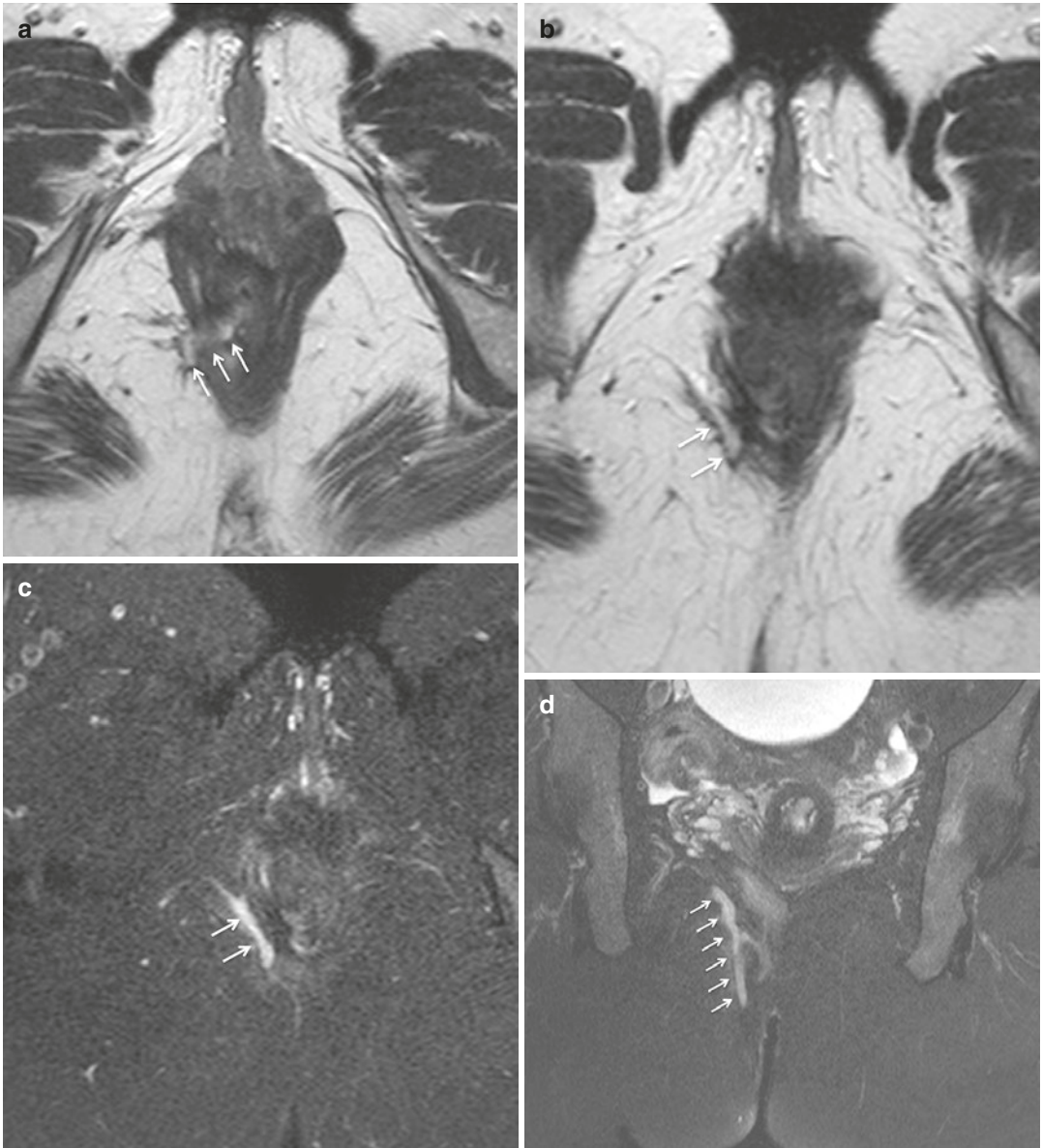
Fig. 9.10 Trans-sphincteric fistula. Axial-oblique T2-weighted TSE image (**a**), showing the internal opening of fistula at 7 o'clock (arrows). More caudally, T2-weighted TSE images, performed without (**b**) and with fat saturation (**c**), show a fistulous tract in the right ischioanal fossa (arrows). Coronal-oblique T2-weighted TSE fat-saturated image (**d**) clearly traces the craniocaudal extent of fistula (arrows)

Fig. 9.11 Perianal abscess. Axial-oblique (**a**), coronal-oblique (**b**), and sagittal (**c**) T2-weighted TSE images show a voluminous perianal abscess (arrows) that displaces to the right side of the sphincteric complex (asterisks)
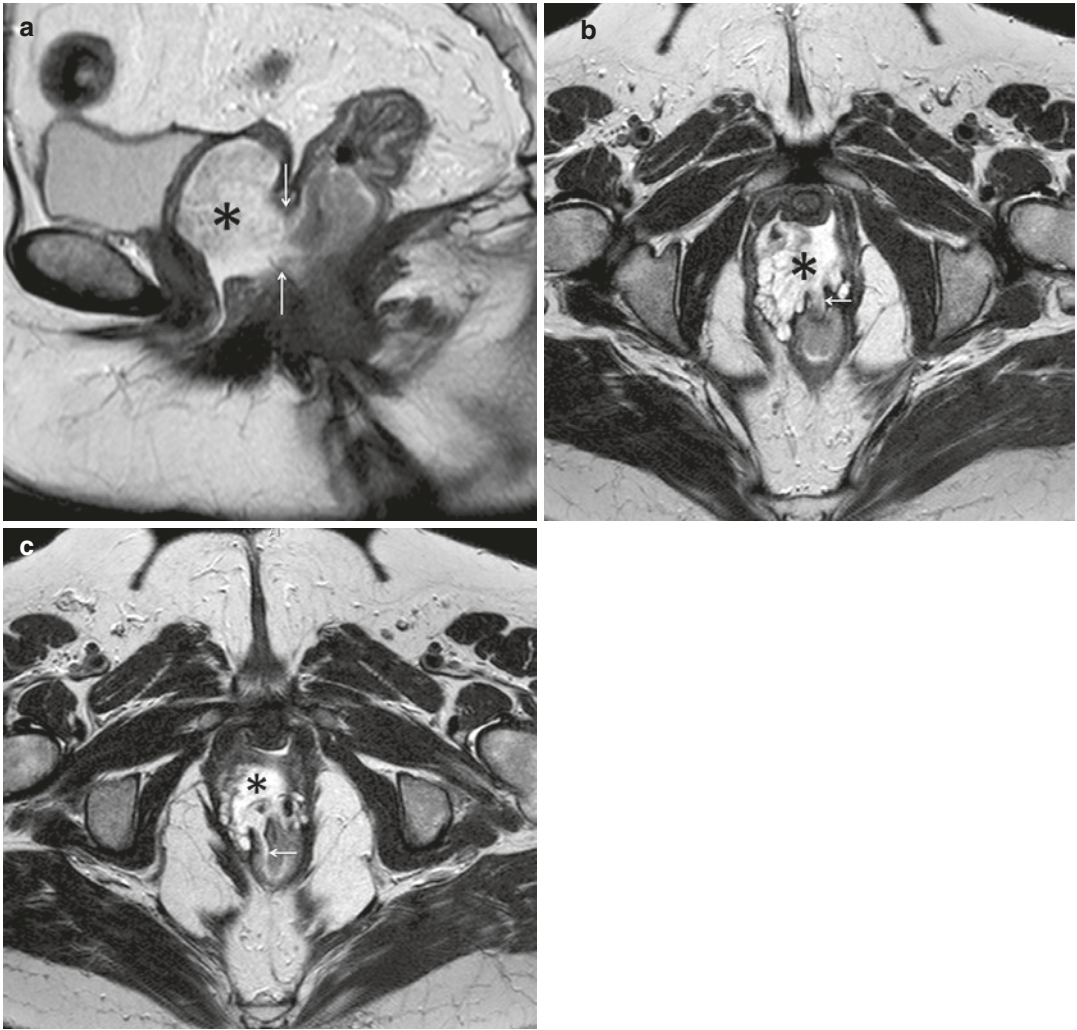
Fig.   9.12 Recto-vaginal   communication. Hysterectomized patient. Sagittal (**a**) and axial-oblique (**b**, **c**) T2-weighted TSE images clearly depict a wide defect of the posterior vaginal wall (arrows in a). On axial-oblique images (**b**, **c**) some fistulous tracts demonstrate a communication with the anterior wall of rectum (arrows). Vaginal lumen is filled with fecaloid material (asterisk)

9.4 MRI of the Anal Canal beyond Crohn's Disease

A number of diseases can take place within the perianal region.

Beyond congenital malformations, they can be grouped into three main types: inflammatory conditions, benign, and malignant lesions.

MRI protocol is the same used for evaluation of fistula-in-ano generally performed in CD patients.

The main purpose of the exam is to distinguish CD involvement of the anal canal and perianal structures from a different pathology.

9.4.1 Inflammatory Conditions

9.4.1.1 Pilonidal Sinus
Pilonidal sinus derives from a folliculitis at the intergluteal natal cleft and leads to the formation of a sinus tract or abscess [20, 25–27].

It is typically located within the subcutaneous soft tissues near the sacrum or the coccyx and it is characterized by hyperintensity on T2-weighted images [28].

Differential diagnosis includes fistula-in-ano, unlike which no involvement of the sphincteric space nor communication with the anal lumen can be detected [20, 25–28].

9.4.1.2 Hidradenitis Suppurativa
Hidradenitis suppurativa is caused by a chronic occlusion of cutaneous hair follicles of apocrine sweat glands which lead to recurrent inflammations, sinus tract and abscesses formation, and fibrosis [20, 26, 27].

The perineum represents the typical localization in males, whereas the axillae are in females [25].

Inflamed structures appear hyperintense on T2-weighted sequences, particularly on the fat-saturated ones, and surrounded by edema of the adjacent fat tissue [20, 26].

Contrast medium injection may be helpful in demonstrating rim enhancement of abscessual collections [25].

Differentiation from perianal involvement in CD patients may be challenging, since the two conditions may coexist [25].

Extensive bilateral involvement, absence of rectal wall thickening, and lack of communication with the anal canal are findings suggestive of hidradenitis suppurativa [25, 26].

9.4.1.3 Fournier Gangrene
Fournier gangrene is a urological emergency consisting of necrotizing fasciitis of the genitourinary, perineal, and perianal tissues caused by infection of both aerobic and anaerobic bacteria.

Common causes are traumas or perianal fistulas, although etiology may remain unclear in some cases. Risk factors include diabetes mellitus, obesity, and immunodeficiency.

This condition is burdened by high mortality rates. Death may occur mainly due to sepsis and multiple organ failure [29, 30].

MRI takes advantage of high soft-tissue contrast resolution and a wide field of view.

Moreover, the performance of DWI scans allows recognition of high cellular-density processes, such as abscesses, without any need for intravenous contrast medium injection.

Hence, MRI can be successfully applied not only for initial diagnosis but also during follow-up in order to evaluate treatment outcomes, although its role is usually limited due to prolonged scan times and usual lower scanner availability.

9.4.2 Benign Lesions

Benign lesions of the perianal region can be grossly divided into cystic and fat containing.

Epidermoid and dermoid cysts arise from the ectoderm. While the formers usually appear as unilocular fluid-filled lesions, the latter are more heterogeneous at MRI due to entrapment of ectodermal elements.

As dermoid cysts, also enteric developmental cysts are characterized by inhomogeneous signal intensity. They represent rare congenital malformations of the developing digestive tract and are of endodermal origin [28].

Fat-containing lesions include lipomas and teratomas.

Lipomas are characterized by homogeneous hyperintensity on T1-weighted images with drop of signal on fat-saturated scans [28].

On the other hand, the adipose content within presacral teratoma is lower since fluid and solid components usually coexist. Moreover, intralesional septations and calcifications are not rare [28, 31].

9.4.3   Malignant Neoplasms

Anal canal carcinomas represent only a small percentage (2.5%) of the whole colorectal carcinomas [25, 26, 32].

The main histological type is squamous cell carcinoma (SSC; 80–85%), whereas the remaining include adenocarcinomas, melanomas, lymphoma, GI stromal tumor, and leiomyosarcomas [25, 26, 32].

Risk factors for SCC occurrence are chronic infection with human papillomavirus, in particular 16 and 18 types, human immunodeficiency virus (HIV), infections, and immunosuppression [25, 32].

Resort to MRI is necessary for local staging, including tumor size, sphincteric infiltration, and lymph nodal spread.

At MRI, SCC shows itself as a lobulated intraluminal or infiltrative mass characterized by iso/hypointense on T1-weighted images, iso/hyperintense on the T2-weighted ones, enhancement after intravenous contrast agent injection, and water restriction on DWI scans [25, 26, 32].

References

1. Schwartz DA, Pemberton JH, Sandborn WJ. Diagnosis and treatment of perianal fistulas in Crohn disease. Ann Intern Med. 2001;135:906–18.
2. Makowiec F, Jehle EC, Becker HD, et al. Perianal abscess in Crohn's disease. Dis Colon Rectum. 1997;40:443–50.
3. Rankin GB, Watts HD, Melnyk CS, et al. National cooperative Crohn's disease study: extraintestinal manifestations and perianal complications. Gastroenterology. 1979;77:914–20.
4. Williams DR, Coller JA, Corman ML, et al. Anal complications in Crohn's disease. Dis Colon Rectum. 1981;24:22–4.
5. Buchmann P, Keighley MR, Thompson H, et al. Natural history of perianal Crohn's disease. Ten year follow-up: a plea for conservatism. Am J Surg. 1980;140:642–4.
6. van Dongen LM, Lubbers EJ. Perianal fistulas in patients with Crohn's disease. Arch Surg. 1986;121:1187–890.
7. Goebell H. Perianal complications in Crohn's disease. Neth J Med. 1990;37(Suppl 1):S47–51.
8. Fielding JF. Perianal lesions in Crohn's disease. J R Coll Surg Edinb. 1972;17:32–7.
9. American Gastroenterological Association. AGA technical review on perianal Crohn's disease. Gastroenterology. 2003;125:1508–30.
10. Hellers G, Bergstrand O, Ewerth S, et al. Occurrence and outcome after primary treatment of anal fistulae in Crohn's disease. Gut. 1980;21:525–7.
11. Safar B, Sands D. Perianal Crohn's disease. Clin Colon Rectal Surg. 2007;20:282–93.
12. Parks A. The pathogenesis and treatment of fistula-in-ano. Br Med J. 1961;1:463–9.
13. Lockhart-Mummery HE. Symposium. Crohn's disease: anal lesions. Dis Colon Rectum. 1975;18:200–2.
14. Alabaz O, Weiss EG. Anorectal Crohn's disease. In: Beck D, Wexner SD, editors. Fundamentals of anorectal surgery. 2nd ed. Philadelphia: WB Saunders; 1999. p. 498–509.
15. Maccioni F, Colaiacomo MC, Stasolla A, et al. Value of MRI performer with phased-array coil in the diagnosis and pre-operative classification of perianal and anal fistula. Radiol Med. 2002;104:58.
16. Parks AG, Gordon PH, et al. A classification of fistula-in-ano. Br J Surg. 1976;63:1–12.
17. Morris J, Spencer JA, Ambrose NS. MR imaging classification of perianal fistulas and its implications for patient management. Radiographics. 2000;20(3):623–35.; discussion 635-7 PMID: 10835116. https://doi.org/10.1148/radiographics.20.3.g00mc15623.
18. Whiteford MH, Kilkenny J 3rd, Hyman N, Buie WD, Cohen J, Orsay C, Dunn G, Perry WB, Ellis CN, Rakinic J, Gregorcyk S, Shellito P, Nelson R, Tjandra JJ, Newstead G, Standards Practice Task Force, American Society of Colon and Rectal Surgeons. Practice parameters for the treatment of perianal abscess and fistula-in-ano (revised). Dis Colon Rectum. 2005;48(7):1337–42. https://doi.org/10.1007/s10350-005-0055-3. PMID: 15933794
19. Sheedy SP, Bruining DH, Dozois EJ, Faubion WA, Fletcher JG. MR imaging of perianal Crohn disease. Radiology. 2017;282(3):628–45. https://doi.org/10.1148/radiol.2016151491. PMID: 28218881
20. Cicero G, Ascenti G, Blandino A, Pallio S, Abate C, D'Angelo T, Mazziotti S. Magnetic resonance imaging of the anal region: clinical applications. J Clin Imaging Sci. 2020;10:76. https://doi.org/10.25259/JCIS_180_2020. PMID: 33274120; PMCID: PMC7708963

21. de Miguel CJ, del Salto LG, Rivas PF, del Hoyo LF, Velasco LG, de las Vacas MI, Marco Sanz AG, Paradela MM, Moreno EF. MR imaging evaluation of perianal fistulas: spectrum of imaging features. Radiographics. 2012;32(1):175–94. https://doi.org/10.1148/rg.321115040. PMID: 22236900

22. O'Malley RB, Al-Hawary MM, Kaza RK, Wasnik AP, Liu PS, Hussain HK. Rectal imaging: part 2, Perianal fistula evaluation on pelvic MRI—what the radiologist needs to know. AJR Am J Roentgenol. 2012;199(1):W43–53. https://doi.org/10.2214/AJR.11.8361. PMID: 22733931

23. Halligan S, Stoker J. Imaging of fistula in ano. Radiology. 2006;239(1):18–33. https://doi.org/10.1148/radiol.2391041043. PMID: 16567481

24. Cicero G, Mazziotti S. Crohn's disease at radiological imaging: focus on techniques and intestinal tract. Intest Res. 2021;19(4):365–78. https://doi.org/10.5217/ir.2020.00097. Epub 2020 Nov 25. PMID: 33232590; PMCID: PMC8566824

25. Erlichman DB, Kanmaniraja D, Kobi M, Chernyak V. MRI anatomy and pathology of the anal canal. J Magn Reson Imaging. 2019;50(4):1018–32. https://doi.org/10.1002/jmri.26776. Epub 2019 May 22. PMID: 31115134

26. Balcı S, Onur MR, Karaosmanoğlu AD, Karçaaltıncaba M, Akata D, Konan A, Özmen MN. MRI evaluation of anal and perianal diseases. Diagn Interv Radiol. 2019;25(1):21–7. https://doi.org/10.5152/dir.2018.17499. PMID: 30582572; PMCID: PMC6339630

27. Erden A. MRI of anal canal: normal anatomy, imaging protocol, and perianal fistulas: part 1. Abdom Radiol (NY). 2018;43(6):1334–52. https://doi.org/10.1007/s00261-017-1305-2. PMID: 28840368

28. O'Neill DC, Murray TE, Thornton E, Burke J, Dunne R, Lee MJ, Morrin MM. Imaging features of benign perianal lesions. J Med Imaging Radiat Oncol. 2019;63(5):617–23. https://doi.org/10.1111/1754-9485.12934. Epub 2019 Aug 1. PMID: 31368659

29. El-Qushayri AE, Khalaf KM, Dahy A, Mahmoud AR, Benmelouka AY, Ghozy S, Mahmoud MU, Bin-Jumah M, Alkahtani S, Abdel-Daim MM. Fournier's gangrene mortality: a 17-year systematic review and meta-analysis. Int J Infect Dis. 2020;92:218–25. https://doi.org/10.1016/j.ijid.2019.12.030. Epub 2020 Jan 18. PMID: 31962181

30. Levenson RB, Singh AK, Novelline RA. Fournier gangrene: role of imaging. Radiographics. 2008;28(2):519–28. https://doi.org/10.1148/rg.282075048. PMID: 18349455

31. Tappouni RF, Sarwani NI, Tice JG, Chamarthi S. Imaging of unusual perineal masses. AJR Am J Roentgenol. 2011;196(4):W412–20. https://doi.org/10.2214/AJR.10.4728. PMID: 21427305

32. Erden A. MRI of anal canal: common anal and perianal disorders beyond fistulas: part 2. Abdom Radiol (NY). 2018;43(6):1353–67. https://doi.org/10.1007/s00261-017-1306-1.